Slagging Behavior of Straw and Corn Stover and the Fate of Potassium under Entrained-Flow Gasification Conditions

S. Leiser
M.K. Cieplik
R. Smit

February 2013
ECN-W--13-002

energy&fuels

Article

pubs.acs.org/EF

Slagging Behavior of Straw and Corn Stover and the Fate of Potassium under Entrained-Flow Gasification Conditions

Simon Leiser,* Mariusz K. Cieplik, and Ruben Smit

Energy Research Centre of The Netherlands (ECN), Post Office Box 1, 1755 ZG Petten, The Netherlands

ABSTRACT: The behavior of straw and corn stover (non-food agricultural residues potentially available for power generation) was studied in a lab-scale reactor under entrained-flow gasification conditions typical for existing integrated gasification combined cycle power systems. This experimental work was assisted by a range of ash-specific analyses and thermodynamic modeling to gain insights into both the physics and chemistry of ash formation and melting behavior. It was observed that, although the major part of the primarily siliceous native ash promptly forms a molten slag, much of the alkalis are evaporated into the syngas. These gas-borne alkalis can potentially cause aerosol formation in the gasifier, gas quench, syngas cooler, and quench systems, resulting in both operating problems (fouling) and emission issues. To minimize the alkali release from straw and corn stover, the addition of an additive (clay) has been proven to be a highly promising method without the negative effects for the melting behavior of the slag.

INTRODUCTION

Biomass (co-)firing in coal-based systems appears to be one of the most promising and relatively inexpensive methods for the reduction of the fossil fuels use and the related CO_2 emissions. An important application of coal is the production of syngas through entrained-flow (EF) gasification. Syngas is a key intermediate product for a wide range of energy carriers and products, e.g., power, fuels, chemical products, substitute natural gas, and hydrogen. Through biomass co-firing or, in other words, replacing coal with biomass, the CO_2 emissions of all downstream products are decreased. One of the early markets for biomass-based syngas production is power production. The application of woody biomass at high co-firing percentages with coal or even repowering with pure biomass has become a daily practice in the power industry throughout the world. Most of the current co-firing is performed in modern coal-fired pulverized-fuel (PF) and fluidized-bed (FB) boilers. This has proven to be relatively straightforward because the most popular fuels are either lean in ash or contain ash that does not melt significantly under the conditions in these types of plants.

Even more so, the current co-firing fuel portfolio is suffering from an ever tighter woody biomass market and rising objections from environmentalists, because the sustainability of wood production is difficult to guarantee and control. Also, it is expected that clean woody biomass will be phased out from the power industry and used as the feedstock for second- and third-generation biofuels because this is a product with a higher value than heat and power. Therefore, there is a growing interest in the application of alternative feedstocks, for both power generation and the production of transportation fuels.

Agriculture residues and fast-growing grassy biomasses have been identified as a good alternative for wood from a sustainability point of view. One of the main reasons for the interest in these types of biomass is their worldwide availability. The main source are byproducts from the food industry, which are available in relatively large quantities and do not compete with food production. However, these materials, which include several types of straw, a range of palm oil residues, and corn residues, have physical and chemical properties that are widely different from those of wood. The most important difference is the much higher ash content compared to wood. Second, this high content of ash is highly alkaline and rich in chlorine, which is prone to cause operating problems when used at higher shares for co-firing in existing coal PF infrastructure, especially with respect to slagging, fouling, and corrosion.[1−5] However, the low melting temperatures of the ashes make these fuels potentially well-suited for slagging thermal conversion systems in which slag formation on the gasifier walls is essential for the save operation of these kinds of plants.

For the production of syngas from biomasses and biomass co-firing of fuels, such as straw, corn stover, palm oil residues, or other agricultural residues, it is thus of key importance to know what the effects are of ashes in such fuels on the slagging and fouling behavior. After the slagging behavior of woody biomass is investigated with high-temperature melting ash dominated by calcium, with little silicon and potassium,[6] the properties of low melting ashes of straw and corn stover, dominated by silicon, potassium, and chlorine are considered in detail. This is performed by deploying the experimental, analytical, and thermodynamic modeling methodologies established and improved on the basis of the above-mentioned earlier work, thus allowing for a direct comparison of the results. Furthermore, the objective of this work is to demonstrate the usability of kaolin as an additive that reduces alkali release of the fuels into the gas atmosphere while showing little negative impact on the melting behavior of the ash.

EXPERIMENTAL SECTION

Lab-Scale Combustion and Gasification Simulator. Experiments were performed in an electrically heated atmospheric EF reactor [lab-scale combustion and gasification simulator (LCS)] equipped

Received: November 8, 2012
Revised: December 19, 2012
Published: December 20, 2012

with a multi-stage gas burner that has been applied extensively in previous studies of PF combustion and gasification.[6−9] The top section of the LCS is schematically shown in Figure 1. It has been designed to

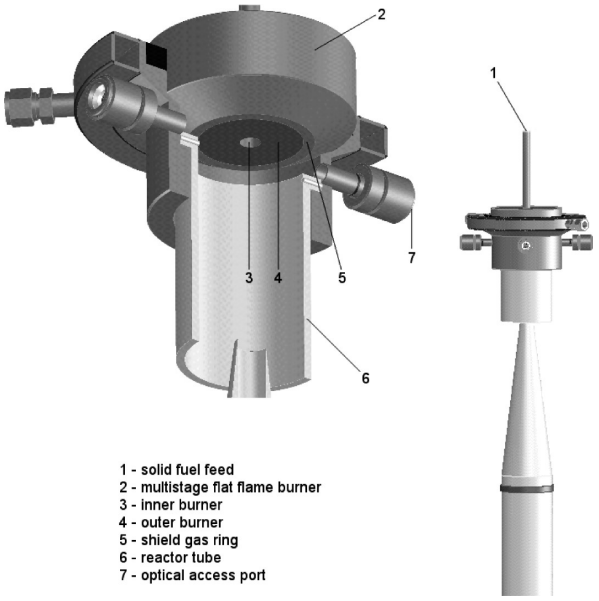

Figure 1. Schematic representation of the top section of the LCS test rig.

mimic PF combustion and dry-fed, oxygen-blown EF gasification conditions in terms of particle heating rates, reaction atmosphere, and temperature−time history. The ring-shaped, concentric, staged gas burner with which solid fuels are fed through the annulus is used to simulate the high initial heating rate, resulting in a very rapid pyrolysis and devolatilization of particles. The outer burner is a flat flame burner that serves as a source for the appropriate reaction atmosphere and pilots the inner burner through which the particles enter the reactor traveling through a premixed Bunsen-like flame. The whole-alumina reactor of approximately 1.2 m in length, placed in a three-stage electrically heated furnace, is designed to further simulate the temperature−time history downstream of the flame front. To create conditions characteristic for EF gasification, very high flame front temperatures are applied (>2250 °C), while the reactor/furnace can be operated at temperatures up to 1700 °C. Because biomass is typically more reactive than coal as a result of the higher volatile/fixed carbon ratio, the experiments have been conducted at a relatively low temperature of 1300 °C, in comparison to typical operating temperatures of coal-fed gasifiers (e.g., 1450 °C and higher). Reducing the operating temperature during biomass gasification offers a number of benefits, which are mainly attributable to the lower energy content of biomass; lowering the gasification temperature will increase the cold-gas efficiency, reduce the oxygen consumption and reduce the CO_2 concentration in the untreated synthesis gas. The latter is important to ease operation of the acid gas removal section, where the minimum H_2S threshold of the acid gas stream to the Claus unit should approximately amount to 25%.[10]

Details of the operating conditions and gas compositions applied to the LCS gas burner are given in Table 1.

Table 1. Gas Burner Flow Rates (L_n/min)

	CH_4	O_2	CO	H_2	N_2
inner burner		0.108	0.947	0.566	0.37
outer burner	2.28	5.13			19
shield gas ring					0.81

Data generated with the LCS were successively validated over the past decade against several full-scale utilities, including a 250 MW_e integrated gasification combined cycle (IGCC) in The Netherlands.

Particulate Sampling. Particulate samples are taken by means of an oil-cooled movable suction probe that is inserted from the bottom of the furnace. Within the probe, the particles are rapidly cooled (quenched) and subsequently collected by either a flat filter (bulk samples) or a cascade impactor (fractionated samples). For this study, Nuclepore polycarbonate filter material was used for both the bulk particle samples and size-resolved cascade impactor sampling. For the latter, a Pilat Mark 5 cascade impactor,[11] which comprises up to 11 separation stages, was used. The characteristic particle diameters d_p of the individual stages are given in Table 2. The suction probe was mounted at a distance of 1150 mm from the burner, corresponding to an ambient temperature of 600 °C.

Table 2. Characteristic Particle Diameters for Each Individual Cascade Impactor Stage

	d_p (μm)
stage 1	5.56
stage 2	4.06
stage 3	1.25
stage 4	0.43
stage 5	0.16
stage 6	0.078
stage 7	0.050
stage 8	0.032
stage 9	0.021
stage 10	0.016

Slag Sampling. The slagging behavior of the ash was characterized by means of a deposition probe (Figure 2), on which an uncooled

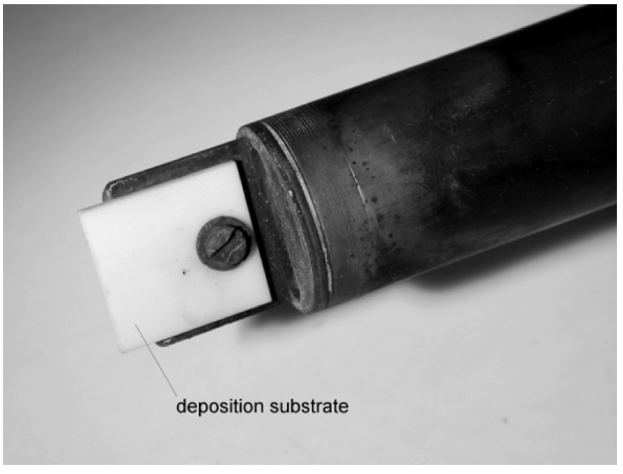

Figure 2. Photograph of the deposition probe with (uncooled) deposition substrate.

alumina deposition plate was mounted on top. This probe was used in numerous studies to evaluate the slagging and fouling behavior of different fuels under combustion and gasification conditions.[6,7] In the present study, the probe was set at two different positions along the reactor axis at distances of 800 and 1150 mm from the gas burner corresponding to temperatures of 1300 and 600 °C, respectively. These temperatures and particle residence times corresponding to the sampling point were chosen to mimic conditions found on the walls of the gasifier (1300 °C) and at the gas quench zone and syngas cooler (600 °C).

Fuels. Experiments in the LCS were carried out using two agricultural residues: straw and corn stover. Ultimate and proximate

dx.doi.org/10.1021/ef301821a | Energy Fuels 2013, 27, 318−326

analyses of the investigated fuels together with the ash composition are given in Table 3.

Table 3. Fuel Analyses

fuel	straw	corn stover
Proximate Analysis		
moisture (%, w/w, ar)	5.01	6.22
volatiles (%, w/w, daf)	80.1	78.68
ash (%, w/w, db)	7.09	10.9
Ultimate Analysis		
C (%, w/w, db)	44.34	42.10
H (%, w/w, db)	5.77	5.61
O (%, w/w, db)	41.54	42.27
N (%, w/w, db)	0.59	0.70
S (%, w/w, db)	0.13	0.07
Cl (%, w/w, db)	0.94	0.19
Mineral Composition		
Al (%, w/w, db)	0.011	0.285
Ca (%, w/w, db)	0.330	0.298
Fe (%, w/w, db)	0.012	0.099
K (%, w/w, db)	1.408	1.350
Mg (%, w/w, db)	0.038	0.113
Na (%, w/w, db)	0.005	0.057
P (%, w/w, db)	0.055	0.068
Si (%, w/w, db)	1.784	2.179

Ash Fusibility. The impact of fluxing on ash fusibility and potassium incorporation was studied by adding commercially available kaolin (CAS 1332-58-7) to fuel ashes produced on a lab scale by a slow, low-temperature ashing method developed at ECN. This method comprises a low heating rate pyrolysis step with a hold time of 24 h at 400 °C and a subsequent slow oxidation of the char at the same temperature. This procedure ensures that particle temperatures remain moderate, so that evaporation of volatile mineral compounds is minimized. The produced ashes are then homogenized by dry sieving using a 53 μm sieve. Also, during this procedure, zirconia balls are placed on the sieve, to break up any larger ash entities.

There are numerous examples of several mineral additives used in the literature,[12−14] however, mostly with the goal of increasing the melting temperature of the ashes, which is undesired in the present case. In this work, kaolin was chosen as the additive for its potassium capture efficiency[15,16] and high reactivity.[13] Kaolin was added to the ashes in portions corresponding to 0.5, 0.9, and 1.2% by weight on a (dry) fuel basis for straw and 0.5, 0.9, and 1.3% by weight on a (dry) fuel basis for corn stover. Subsequently, the pre-blended samples were subjected to ash fusion tests under reducing conditions according to NEN-ISO 540.

Weight Loss and Loss on Ignition (LOI). Char samples were taken in the LCS test rig after a residence time of approximately 2 s using a suction probe and deploying a flat filter. Sample ash was determined according to CEN/TS 14775. The conversion X was then calculated using the ash tracer technique as

$$X = \frac{1 - \frac{\text{ash}_0}{\text{ash}}}{1 - \text{ash}_0}$$

where ash_0 and ash are the ash contents on a dry basis of the initial and gasified samples, respectively. LOI of the gasified sample is given by

$$\text{LOI} = 1 - \text{ash}$$

Thermodynamic Modeling. The fate of alkali metals under EF gasification conditions, in particular that of potassium, was also studied theoretically using a thermodynamic equilibrium model (FACTSage[17,18]). The thermochemical simulation software consists of several thermodynamic property databases and calculation and manipulation modules that can be used to access and combine pure substances and solution databases. When a sophisticated Gibbs energy minimizer and thermodynamic functions are employed,[19] concentrations of chemical species at a given temperature and pressure can be calculated when specified elements or compounds react or partially react to reach the state of chemical equilibrium. The simulations carried out in this work focus on the distribution of potassium in gas, liquid, and solid states at typical operating temperatures of EF gasifiers, corresponding to different regions in the gasifier. Additionally, the effect of adding kaolin as a fluxing agent on the potassium distribution was studied.

The EF gasifier has been modeled as an ideally mixed reactor by introducing a pre-defined amount of fuel and a corresponding amount of oxygen and steam to mimic the operational conditions of a commercial dry-fed, oxygen-blown EF gasifier. The air/fuel ratio (AFR) of 0.25 was chosen for all simulations. For modeling the liquid slag phase, the FACT-SLAGA database was used in all cases.

RESULTS AND DISCUSSION

Ash Fusion Temperatures. Table 4 summarizes the results of the ash fusion tests. Both fuel ashes, without the addition of kaolin, show relatively low melting temperatures in the range of 1200−1300 °C, underlining the feasibility of usage of these fuels under the conditions of a slagging EF gasifier. The addition of kaolin alters the melting behavior of the ashes only marginally. In the case of straw ash, the fluid temperature first decreases with the addition of kaolin, possibly because of the formation of low-melting eutectics, and supersedes the raw ash melting temperature only by 30 °C for the highest flux level of 1.2%. Corn stover ash seems not to be prone to form low-melting eutectics with kaolin, and consequently, the fluid temperature increases with an increasing flux level because of the higher melting point of kaolin of approximately 1750 °C. However, the fluid temperature for the highest flux level of 1.3% only increases by 130 °C to a temperature of 1330 °C. This latter temperature remains still sufficiently low for the application in the temperature range of a slagging gasifier. It should be noted that the prediction of the slagging and fouling behavior of fuel ashes based on the ash fusion test has a number of drawbacks, particularly so because the absolute melting temperatures determined may not quantitatively represent the whole range of melting behavior correctly, especially the onset of sintering and melting represented by the deformation temperature.[20] However, because a slagging EF gasifier requires

Table 4. Measured Ash Fusion Temperatures (°C) of Straw and Corn Stover Ash at Different Fluxing Levels with Kaolin

characteristic temperature[a]	straw, no additive	straw, 0.5% kaolin	straw, 0.9% kaolin	straw, 1.2% kaolin	corn stover, no additive	corn stover, 0.5% kaolin	corn stover, 0.9% kaolin	corn stover, 1.3% kaolin
DT	1000	1050	1080	1080	960	1090	1150	1160
ST	1080	1100	1140	1190	1050	1180	1240	1280
HT	1140	1150	1200	1260	1120	1230	1270	1300
FT	1280	1200	1250	1310	1200	1290	1320	1330

[a]DT, deformation temperature; ST, softening temperature; HT, hemisphere temperature; FT, fluid temperature.

dx.doi.org/10.1021/ef301821a | Energy Fuels 2013, 27, 318−326

a running slag, the fluid temperature is of greater importance. Furthermore, the tests were intended to investigate and demonstrate the impact of kaolin addition to the fuel ashes on the melting behavior, which has been shown to have a minor negative impact.

Fuel Reactivity. Both investigated fuels were characterized in terms of conversion at the given residence time of approximately 2 s by means of particle sampling at the reactor outlet and subsequent determination of combustible conversion using the ash tracer technique. Table 5 summarizes the results.

Table 5. Conversion of Straw and Corn Stover in the LCS Test Rig

fuel	straw	corn stover
conversion (%, w/w, daf)	99.67	99.73
LOI (%, w/w, db)	4.54	2.21

It can be seen that the carbon conversion of the fuels at the conditions applied is almost complete and should hence not cause any problems in real systems.

Fractionated Ash Samples. Particle samples of straw ash were taken at the same location as the samples obtained for conversion determination using a Pilat Mark 5 cascade impactor. Impactor stages were weighted and analyzed for particle morphology and chemical composition by means of scanning electron microscopy coupled with energy-dispersive X-ray (SEM−EDX). The results of the latter analysis are summarized in Figure 3. In the first stages, i.e., for particle sizes

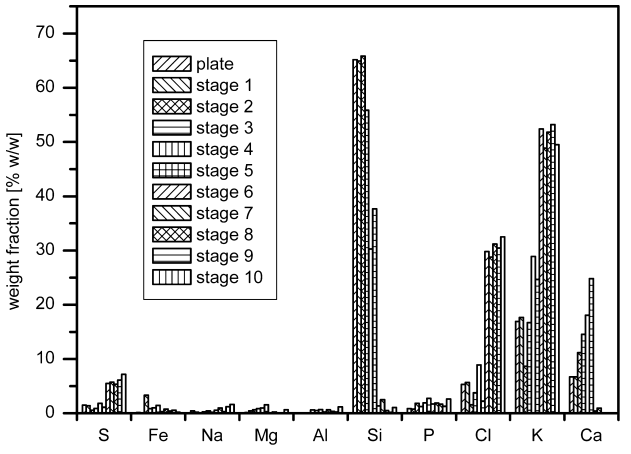

Figure 3. Mineral composition of straw ash/char particles for different size classes. Component fractions are given as carbon- and oxygen-free bases.

larger than 1 μm (impactor plate and stages 1, 2, and 3), large fibrous char/ash structures with large pores were obtained with clearly distinguishable particle agglomerates on the surface, as shown in Figure 4. Elemental analysis revealed that the mineral fraction of the large particles was mainly composed of SiO_2 with small amounts of potassium, as shown in Table 6. The smaller particulate agglomerates on the char/ash surfaces appear to be (originally gas-borne) precipitates of potassium salts (KOH, KCl, and K_2SO_4), with small fractions of silicon oxide (measurement point a in Figure 4). Most likely silicon oxides acted as condensation nuclei for the potassium salts.

In the successive impactor stages (starting from stage 4 onward), where sub-micrometer particles (and/or their

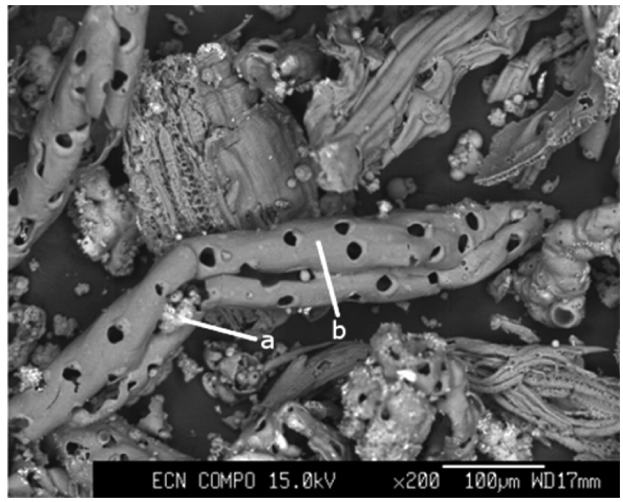

Figure 4. SEM micrograph taken from straw ash/char particles collected at the first stage of the cascade impactor (probe position at 1150 mm from the burner, with a gas temperature of 600 °C).

agglomerates) are impacted, the elemental analysis reveals that almost exclusively potassium salts are collected. As an example, Figure 5 shows particulate matter collected at the sixth stage of the cascade impactor. Remarkably, the composition of this sample differs only marginally from the sample obtained from the extra-char/ash particulate described above (see Table 6, measurement point a in Figure 4). This clearly underlines the hypothesis that particles originate from condensed potassium salts. This appears to be more obvious for the crystalline structure shown in Figure 5. In summary, it can be concluded that large fractions of K, Cl, and S are released during devolatilization and gasification. These elements condense as sub-micrometer salts at lower temperatures, which can cause severe fouling[4,21] and corrosion[22,23] problems on cooled surfaces of the gasifier and downstream equipment, such as a syngas cooler.

Slagging and Fouling Behavior of Straw. Figure 6 shows the top view of the deposition substrate after a 3 h straw gasification experiment at a distance of 800 mm from the burner. The collected particles show strong sintering and partial melting, indicating that straw ash may form sufficient liquid slag at typical operating conditions of a slagging gasifier, i.e., in the temperature range between 1300 and 1500 °C.

The collected particles are rich in silicon, with smaller quantities of oxygen, potassium, and phosphorus (see measurement point a in Figure 6). With respect to the composition of the sample, silicon oxide, perhaps also partly reduced to silicon carbide, is likely to be the main constituent within the mineral matrix. Furthermore, unlike for the samples taken at the (cold) reactor exit (Figures 4 and 7), no potassium salts on the surface could be found. This implies that temperatures in the range of 1300 °C, where the sample was taken, prohibited nucleation of potassium salts, while only an insignificant fraction could have formed (alumino-)silicates.

Deposits collected at a reduced temperature of approximately 600 °C at a greater distance from the burner (1150 mm) are shown in Figures 7 and 8. The larger fibrous particles impacted on the deposition substrate (see measurement point a in Figure 7) are primarily composed of silicon (oxide) with a smaller fraction of potassium. The latter is for a part incorporated into the slag matrix, while substantial amounts of potassium (as

dx.doi.org/10.1021/ef301821a | Energy Fuels 2013, 27, 318−326

Table 6. SEM–EDX Analysis Results

analysis point	a in Figure 4	b in Figure 4	Figure 5	a in Figure 6	a in Figure 7	b in Figure 7	a in Figure 8	a in Figure 9	b in Figure 9	a in Figure 10	b in Figure 10
fuel	straw	straw	straw	straw	straw	straw	straw	corn stover	corn stover	corn stover	corn stover
O (%, w/w)	15.09	39.16	15.31	9.06	43.37	32.73	2.56	24.93	31.76	36.86	41.10
Al (%, w/w)	0.20	0.00	0.22	0.06	0.12	0.01	0.54	1.95	1.34	5.89	1.49
Ca (%, w/w)	0.33	0.16	0.36	1.01	0.54	9.97	0.72	10.32	9.14	8.58	29.49
Cl (%, w/w)	24.66	0.19	25.25	0.00	0.64	0.01	42.39	0.15	0.05	0.08	0.24
Fe (%, w/w)	0.64	0.09	0.26	0.76	0.18	0.13	0.00	4.92	1.77	10.32	1.37
K (%, w/w)	44.12	3.17	44.38	7.99	11.09	19.87	51.08	13.35	9.69	7.68	6.53
Mg (%, w/w)	0.00	0.12	0.08	0.28	0.15	12.55	0.02	1.45	2.47	6.71	0.52
Na (%, w/w)	1.29	0.30	0.47	0.00	0.07	0.06	0.00	0.94	1.52	0.78	0.28
P (%, w/w)	1.18	0.00	1.45	2.65	0.26	14.99	0.39	0.93	0.73	0.51	6.53
S (%, w/w)	7.48	0.06	4.65	0.00	0.00	0.00	0.00	0.07	0.01	0.06	0.05
Si (%, w/w)	3.35	55.09	1.14	77.85	43.53	9.53	2.29	39.89	40.19	21.33	12.23

Figure 5. SEM micrograph of particulate matter collected in the sixth stage of the cascade impactor during EF gasification of straw (probe position at 1150 mm from the burner, with a gas temperature of 600 °C).

Figure 6. SEM micrograph taken from ash/char particles deposited on an (uncooled) alumina deposit plate (top view) after a 3 h LCS straw gasification test (probe position at 800 mm from the burner, with a gas temperature of 1300 °C).

KCl) have grown crystals on the deposit surface. These structures are likely products of heterogeneous nucleation and/or condensation (see measurement point a in Figure 8). This implies that gaseous potassium would likely form similar deposits on relatively cold surfaces, such as heat exchanger surfaces. This condensation leads to severe fouling problems and reduced heat transfer of a syngas cooler. Additionally, smaller sphere-shaped particles consisting of phosphates and oxides of calcium, potassium, magnesium, and silicon could be retrieved (see measurement point b in Figure 7).

Slagging and Fouling Behavior of Corn Stover. The deposits formed during EF gasification of corn stover at a distance of 800 mm from the burner corresponding to a temperature region of approximately 1300 °C are shown in Figure 9. The collected slag is fully molten but not running. The higher degree of melting compared to straw slag is in agreement with the ash fusion temperatures determined on a lab scale. The slag contains two immiscible phases (indicated as

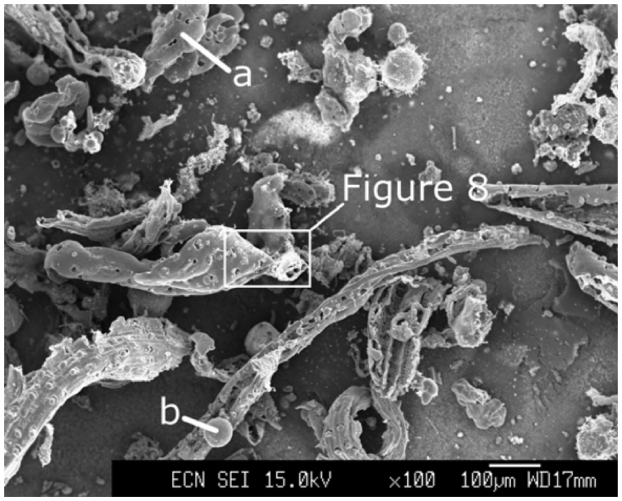

Figure 7. SEM micrograph taken from ash/char particles deposited on an (uncooled) alumina deposit plate (top view) after a 3 h LCS straw gasification test (probe position at 1150 mm from the burner, with a gas temperature of 600 °C).

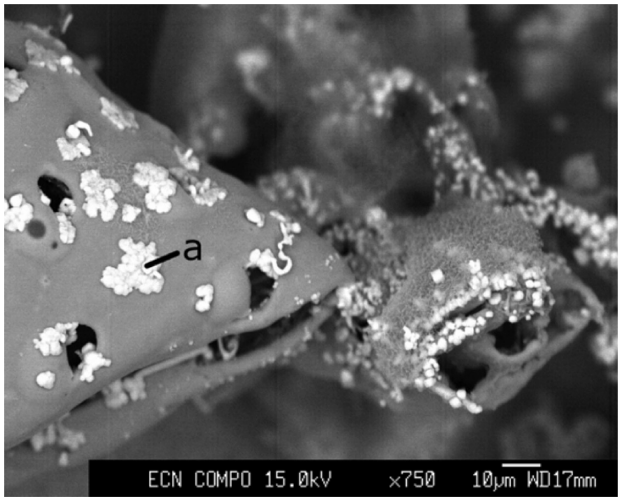

Figure 8. Magnification of Figure 7.

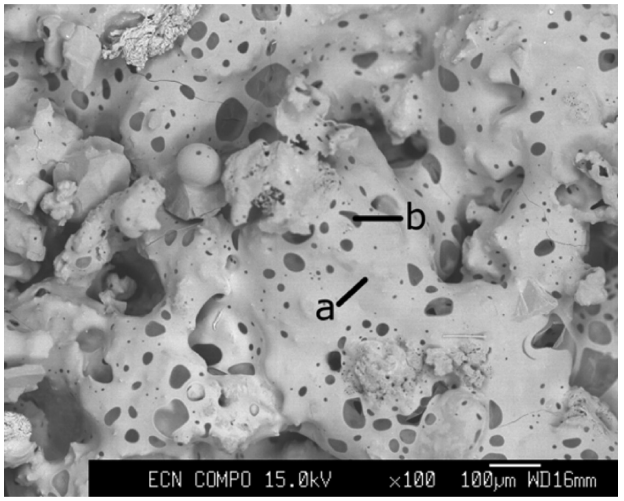

Figure 9. SEM micrograph taken from ash/char particles deposited on an (uncooled) alumina deposit plate (top view) after a 3 h LCS corn stover gasification test (probe position at 800 mm from the burner, with a gas temperature of 1300 °C).

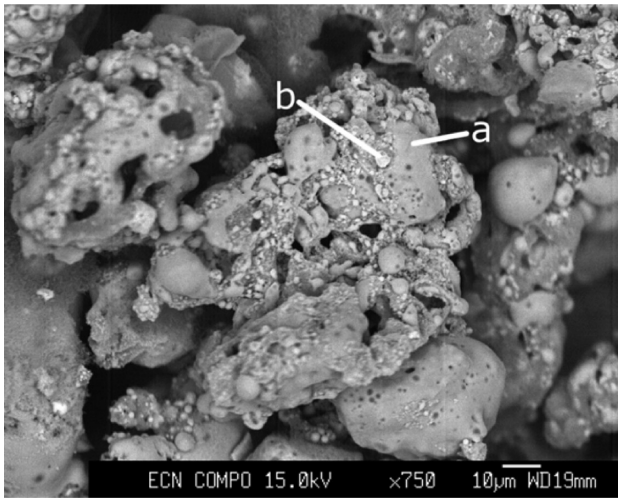

Figure 10. SEM micrograph taken from ash/char particles deposited on an (uncooled) alumina deposit plate (top view) after a 3 h LCS corn stover gasification test (probe position at 1150 mm from the burner, with a gas temperature of 600 °C).

measurement points a and b in Figure 9), which differ in composition mainly for iron, potassium, and oxygen. Similar to the previous case of straw slag, no external potassium-containing precipitates could be detected; however, the potassium concentration in the prevailing slag matrix (measurement point a in Figure 9) is notably higher for corn stover slag than for straw slag.

The top view of the deposit substrate from a corn stover EF gasification test at a burner distance of 1150 mm at a temperature of approximately 600 °C is shown in Figure 10. Also, in this case, the surface of the deposit appears to be far more fused than in the case of straw. However, clearly multiple phases are present. As seen in Table 5, the bulk of the molten/fused particles is rich in silicon, while also iron and, naturally, potassium are present in sizable amounts, accompanied by calcium. The smaller sphere-shaped particles impacted but not dissolved in the slag are much richer in calcium and phosphorus, while the concentration of iron is much lower. Unlike the case of straw, no crystalline or generally potassium-based phases could be seen. This may suggest that stover-bonded potassium is better incorporated into the bulk of the slag and forms larger particles than in the case of straw ash. Furthermore, because of the significantly lower chlorine content of corn stover, it is likely that less potassium is released into the gas phase during pyrolysis and gasification, because the presence of chlorine greatly impacts the release and retention of potassium.[24] This suggests that corn stover may pose less of a threat of potassium aerosol formation under the conditions of EF gasification and less alkali-induced fouling and corrosion.

Thermodynamic Equilibrium Modeling. The distribution of gaseous and condensed phases that bound potassium in either the liquid or solid phase was modeled under atmospheric EF gasification conditions with FACTSage software. Results are shown in Figures 11 and 12 for straw and corn stover, respectively. The results of the simulations indicate that potassium in the gas phase is mainly present as elemental K, KCl, and KOH, while the dominant species in the liquid slag is K_2O. Solid-bound potassium is exclusively found as leucite at

dx.doi.org/10.1021/ef301821a | *Energy Fuels* 2013, 27, 318−326

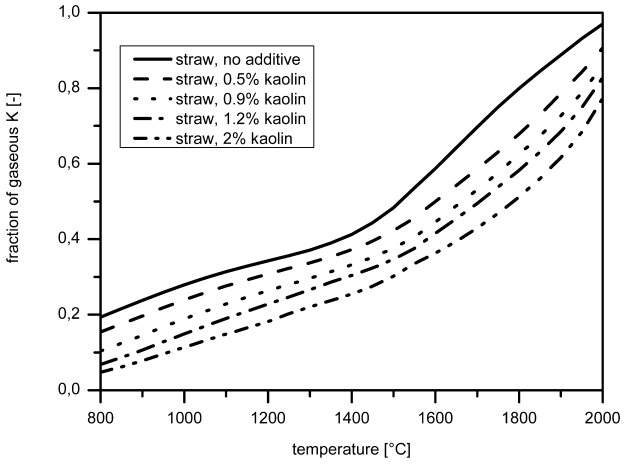

Figure 11. Calculated potassium release of straw under EF gasification conditions for different flux levels as a function of the temperature.

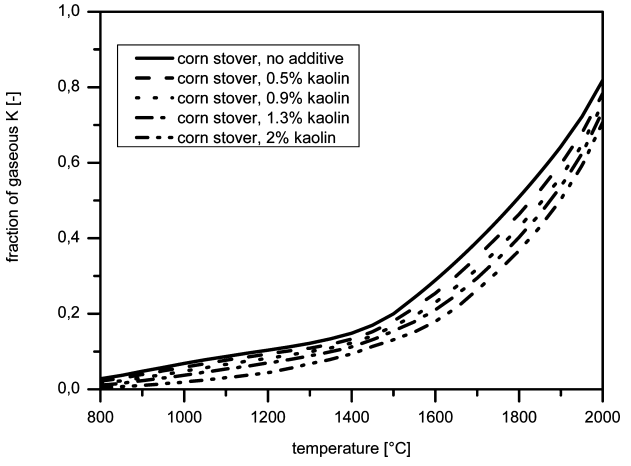

Figure 12. Calculated potassium release of corn stover under EF gasification conditions for different flux levels as a function of the temperature.

higher temperatures (>900 °C), while at lower temperatures, KCl is the dominant species. Supported by the experimental observations, the potassium release of straw is generally higher than for corn stover. This is primarily due to the lower aluminum content of straw, preventing the formation of potassium binding aluminosilicates, such as leucite, and the higher chlorine content of straw. The alkali release modeling is in accordance with the experimental findings of the predicted higher incorporation of potassium into the slag formed from corn stover.

Adding kaolin as a flux at levels lower than 2% (w/w) on a (dry) fuel basis showed also only a slight increase of the melting temperature in the model (data not shown). However, it should be pointed out that the determination of the melting temperature by thermodynamic equilibrium modeling remains problematic. To predict ash melting temperature criteria, such as the temperature when the liquid mineral fraction reaches a certain percentage, Li et al.[25] used a liquid fraction of 75% (w/w), while Coda et al.[6] used a liquid fraction of 70% (w/w). For the fuels investigated in this study, a satisfactory agreement with the measurements was only obtained when a liquid fraction of 80% (w/w) for corn stover and 90% (w/w) for straw was applied. This might be due to shortcomings of the thermodynamic databases incorporated in FACTSage or effects of different slag viscosities that alter the measured values compared to the predicted values.

Potassium incorporation into the slag phase can be significantly improved by fluxing the fuel with kaolin. The impact of flux addition on potassium release calculated with FACTSage is shown in Figures 13 and 14 as the mass fraction

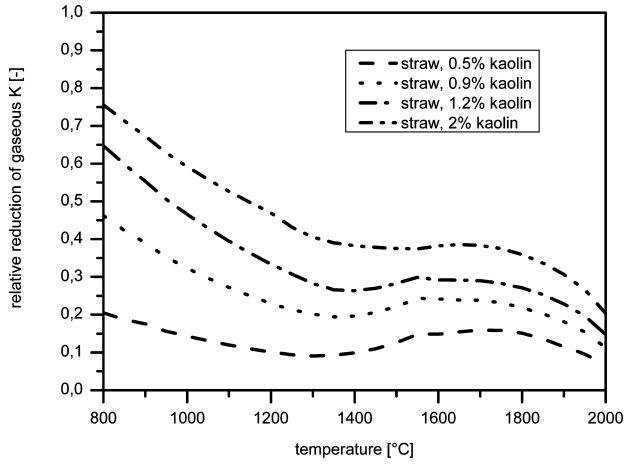

Figure 13. Impact of flux addition on potassium release of straw under EF gasification conditions. Reduction of gaseous potassium is based on calculated initial release without the addition of kaolin.

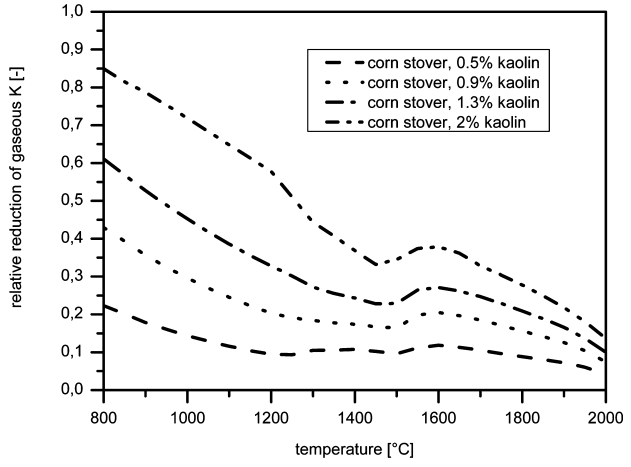

Figure 14. Impact of flux addition on potassium release of corn stover under EF gasification conditions. Reduction is based on calculated initial release without the addition of kaolin.

of gaseous potassium referred to the total mass. The highest flux level of 2% (w/w) was used as a reference of the upper limit of technically and economically feasible flux addition. However, in the latter case, the melting temperature would increase excessively, leading to insufficient amounts of liquid slag, a situation unacceptable from the operating point of view. For that reason, only flux levels below 2% (w/w) were tested experimentally.

As mentioned earlier, the release of potassium from straw during gasification is generally higher than for corn stover, which can be explained by the lower amounts of aluminosilicates in the slag/ash matrix and the higher chlorine content of straw that facilitates the release of potassium. Within the temperature range relevant for EF, the addition of kaolin reduces the amount of potassium released into the gas phase by up to 30% for a flux of 1.2% (w/w) relative to the release of

dx.doi.org/10.1021/ef301821a | Energy Fuels 2013, 27, 318−326

potassium from the unfluxed material. Even higher capture efficiencies can be achieved at lower temperatures according to equilibrium modeling. However, it remains questionable whether thermodynamic equilibrium will be reached at lower temperatures within the residence time in an EF gasifier, considering that solid-state chemistry is comparatively slow.

The relative reduction of gaseous potassium by the addition of kaolin in the case of corn stover gasification is slightly lower than for straw. However, given the lower initial release of the unfluxed material, the absolute potassium retention in the ash/slag matrix is significantly higher than for straw.

CONCLUSIONS AND OUTLOOK

EF oxygen-blown slagging gasifiers are one of the key technologies for high-efficient syngas production. Important applications of EF gasification are high-efficiency power generation (IGCC), fertilizer production, and transportation fuel production via Fischer−Tropsch. However, the EF gasifiers that are currently on the market have been designed for coal and its specific characteristics, such as conversion/residence time, but also ash composition, especially in terms of alkali and alkaline earth metals. Biomass has the potential to replace coal and reduce the CO_2 emissions from the applications of EF gasification. Hence, to enable the use of agricultural residues as fuels for EF slagging gasifiers, some important challenges that are mainly related to the fuel reactivity and the slagging behavior of the ashes need to be overcome. In this paper, the effects on using the agricultural residues straw and corn stover in an EF gasifier have been investigated. The relatively high concentrations of alkalis in these fuels, particularly potassium, may also cause severe slagging and fouling problems in the cooling section of an EF slagging gasifier. For this reason, the fate of alkalis needs to be tackled in a detailed way. The characterization has been performed by a combination of lab-scale experimental and modeling work.

Lab-scale EF gasification experiments have been carried out using straw and corn stover. Both are typical dry arable crop residues, available in relatively large quantities on the market. Conversion tests performed at wall temperatures of 1300 °C and a reaction atmosphere representative for EF gasification showed essentially full conversion of the fuels after a residence time of 2 s, giving indications that the size of an EF slagging gasifier dedicated to biomass conversion may have smaller dimensions than a model designed for operation with coal.

Under the same reactor conditions, slagging measurements were performed in the high-temperature region of the LCS reactor and at the LCS reactor exit, where gas temperatures are comparable to the cooling section of an EF gasifier. In the high-temperature zone, straw slag samples have shown to contain only small fractions of potassium and consisted mainly of siliceous phases. In the low-temperature regime, condensed potassium chloride crystals and agglomerates were observed on the surface of larger straw ash/slag particles. The results from fractionated cascade impactor ash samples, taken at the reactor outlet, have revealed that potassium (salt) is found predominantly in the gas phase at high temperatures and forms submicrometer particles when cooled. This leads to the conclusion that sub-micrometer particles (aerosols) potentially cause severe slagging and fouling problems in the cooling section of an EF gasifier.

Test runs with corn stover under the same set of conditions yielded similar results. However, because of a different ash composition, in particular with respect for the presence of aluminosilicates, and a significantly lower chlorine content as compared to straw, a higher amount of potassium was bound into the ash/slag matrix. Nonetheless, a substantial amount of potassium-containing species remained in the gas phase and formed fine particulate matter upon cooling.

The impact of using kaolin as a (model) fluxing agent was studied experimentally and theoretically. Experimental results revealed that employing kaolin up to a fuel-based mass fraction of 1.2−1.3% (w/w) does not increase the melting temperature of straw and corn stover ash significantly, maintaining the typical temperature requirements of an EF slagging gasifier.

Theoretical assessment of fluxing strategies by means of thermodynamic equilibrium modeling shows that kaolin can be applied to efficiently bind potassium in the high-temperature regime, hence lowering the downstream fouling propensity because of potassium-salt-induced aerosol formation. Simulation results also indicate that by decreasing the gasification temperature even higher amounts of potassium could be bound and potassium aerosol could be decreased even more. However, it remains questionable whether thermodynamic equilibrium could be reached within the given residence time in a gasifier at temperatures lower than 1000 °C.

Further research work is required to quantitatively assess the incorporation of alkalis into ashes and slags. Kinetic studies should be carried out to gain a deeper understanding of the physicochemical nature of the problem and to provide advice for the design of new generation EF slagging gasifiers using biomass feedstocks.

AUTHOR INFORMATION

Corresponding Author

*Telephone: +31-224-568078. Fax: +31-224-568487. E-mail: leiser@ecn.nl.

Notes

The authors declare no competing financial interest.

ACKNOWLEDGMENTS

We thank Peter Heere for his deep involvement in carrying out the experimental part of this work.

REFERENCES

(1) Werther, J.; Saenger, M.; Hartge, E. U.; Ogada, T.; Siagi, Z. *Prog. Energy Combust. Sci.* **2000**, *26*, 1−27.

(2) Jenkins, B. M.; Baxter, L. L.; Miles, J.; Miles, T. R. *Fuel Process. Technol.* **1998**, *54*, 17−46.

(3) Natarajan, E.; Nordin, A.; Rao, A. N. *Biomass Bioenergy* **1998**, *14*, 533−546.

(4) Xu, X. G.; Li, S. Q.; Li, G. D.; Yao, Q. *Energy Fuels* **2009**, *24*, 241−249.

(5) Andersen, K. H.; Frandsen, F. J.; Hansen, P. F. B.; Wieck-Hansen, K.; Rasmussen, I.; Overgaard, P.; Dam-Johansen, K. *Energy Fuels* **2000**, *14*, 765−780.

(6) Coda, B.; Cieplik, M. K.; de Wild, P.; Kiel, J. H. A. *Energy Fuels* **2007**, *21*, 3644.

(7) Korbee, R.; Boersma, A. R.; Cieplik, M. K.; Heere, P. G. T.; Slort, D. J.; Kiel, J. H. A. *Fuel Characterisation and Test Methods for Biomass Co-firing; Contribution to EU Project ENKS-1999-00004 Combustion Behaviour of "Clean" Fuels in Power Generation (BioFlam)*; ECN: Petten, The Netherlands, 2003; ECN-C-03-057.

(8) Kiel, J. H. A.; Eenkhoorn, S.; Heere, P. G. T. *Ash Behaviour in Entrained-Flow Gasification: Preliminary Studies*; ECN: Petten, The Netherlands, 1999; ECN-C-99-037.

(9) Dacombe, P. J.; Jacobs, J. M.; Kiel, J. H. A. *Ash Formation in Entrained Flow Co-gasification of Coal and Biomass; ECN Contribution*

to the ECSC Project "Slag Building Behaviour during Entrained Bed Coal Gasification (SLABE)"; ECN: Petten, The Netherlands, 2003; ECN-CX-03-033.
(10) Higman, C.; Burgt, M. v. d. *Gasification*, 2nd ed.; Elsevier: Amsterdam, The Netherlands, 2008.
(11) Pilat, M. J.; Steig, T. W. *Atmos. Environ.* **1983**, *17*, 2429−2433.
(12) Risnes, H.; Fjellerup, J.; Henriksen, U.; Moilanen, A.; Norby, P.; Papadakis, K.; Posselt, D.; Sörensen, L. H. *Fuel* **2003**, *82*, 641−651.
(13) Llorente, M. J. F.; Arocas, P. D. a.; Nebot, L. G. r.; García, J. E. C. *Fuel* **2008**, *87*, 2651−2658.
(14) Xiong, S.; Burvall, J.; Oerberg, H.; Kalen, G.; Thyrel, M.; Oehman, M.; Bostroem, D. *Energy Fuels* **2008**, *22*, 3465−3470.
(15) Steenari, B. M.; Lindqvist, O. *Biomass Bioenergy* **1998**, *14*, 67−76.
(16) Wei, X.; Schnell, U.; Hein, K. R. G. *Fuel* **2005**, *84*, 841−848.
(17) Bale, C. W.; Chartrand, P.; Degterov, S. A.; Eriksson, G.; Hack, K.; Ben Mahfoud, R.; Melançon, J.; Pelton, A. D.; Petersen, S. *CALPHAD: Comput. Coupling Phase Diagrams Thermochem.* **2002**, *26*, 189−228.
(18) Bale, C. W.; Belisle, E.; Chartrand, P.; Decterov, S. A.; Eriksson, G.; Hack, K.; Jung, I. H.; Kang, Y. B.; Melanton, J.; Pelton, A. D.; Robelin, C.; Petersen, S. *CALPHAD: Comput. Coupling Phase Diagrams Thermochem.* **2009**, *33*, 295−311.
(19) Eriksson, G.; Hack, K. *Metall. Trans. B* **1990**, *21B*, 1013−1023.
(20) Gilbe, C.; Lindstroem, E.; Backman, R.; Samuelsson, R.; Burvall, J.; Oehman, M. *Energy Fuels* **2008**, *22*, 3680−3686.
(21) Nielsen, H. P.; Baxter, L. L.; Sclippab, G.; Morey, C.; Frandsen, F. J.; Dam-Johansen, K. *Fuel* **2000**, *79*, 131−139.
(22) Tillman, D. A.; Duong, D.; Miller, B. *Energy Fuels* **2009**, *23*, 3379−3391.
(23) Blomberg, T. *Biomass Bioenergy* **2012**, 2012.
(24) Johansen, J. M.; Jakobsen, J. G.; Frandsen, F. J.; Glarborg, P. *Energy Fuels* **2011**, *25*, 4961−4971.
(25) Li, H.; Yoshihiko, N.; Dong, Z.; Zhang, M. *Chin. J. Chem. Eng.* **2006**, *14*, 784−789.

ECN
Westerduinweg 3
1755 LE Petten
The Netherlands

P.O. Box 1
1755 LG Petten
The Netherlands

T +31 88 515 4949
F +31 88 515 8338
info@ ecn.nl
www.ecn.nl